Dynamic Pilot Allocation with Channel Estimation in Closed-Loop MIMO-OFDM Systems

Li (Alex) Li, Rodrigo C. de Lamare, and Alister G. Burr,

Abstract

Dynamic pilot allocation (DPA) for Discrete Fourier Transform (DFT)-based channel estimation in MIMO-OFDM systems with spatial multiplexing can significantly improve the bit error rate (BER) performance compared to systems with uniform pilot allocation (UPA). However the exhaustive search for optimum pilot allocation leads to very high complexity. We devise a MIMO iterative pilot search (MIPS) algorithm applied with different multi-input multi-output orthogonal frequency division multiplexing (MIMO-OFDM) receivers (linear, SIC and ML), which significantly reduces the complexity of DPA. Exact derivations are also given based on the receivers. We also propose a novel stacked vector quantization (SVQ) technique to reduce feedback burdens for DPA in MIMO-OFDM system. Simulation results illustrate that the proposed MIPS algorithm with limited feedback can improve the performance of MIMO-OFDM systems.

I. Introduction

Coherent receiver design for MIMO-OFDM systems requires accurate channel state information (CSI) to achieve a comparable symbol error rate (SER) performance to that with perfect CSI [1]. Pilot-symbol-aided channel estimation (PACE) is the most common approach exploited in OFDM systems. For MIMO-OFDM, the pilot allocation is more complicated than for single-input single-output (SISO)-OFDM, because of the superposition of signals from multiple transmit antennas. A number of methods have been proposed to estimate the channels in the presence of inter-antenna interference [2]–[6] using uniform pilot allocation (UPA). Compared to the techniques shown above, the pilot patterns proposed in [7] is flexible and easily integrated with the conventional OFDM DFT-based channel estimation for SISO-OFDM. Furthermore,

these channel estimators often concentrate on the mean square error (MSE) minimization of channel estimates rather than SER optimization. Although the minimum MSE can be achieved using UPA [8], [9], MSE optimization is not equivalent to SER optimization. It has been shown that the BER performance of linear receivers can be improved through DPA or iterative pilot search based DPA for SISO-OFDM and Alamouti-2×1-OFDM systems [10], [11].

We develop a dynamic pilot allocation (DPA) algorithm for MIMO-OFDM systems with spatial multiplexing. The main idea behind DPA is to allocate the pilots to appropriate subcarriers for arbitrary numbers of transmit and receive antennas. The contributions of this work can be summarised as follows. 1) A DPA algorithm for different MIMO-OFDM receivers (linear, SIC, ML) is presented, and a low complexity error approximation technique is applied to DPA for ML receivers; 2) A reduced complexity DPA with MIPS is presented; 3) An SVQ scheme for DPA is proposed to reduce the feedback overhead and the number of search trials, and the SVQ scheme is robust to the delays and errors of the feedback channels. 4) We have also discussed the selection diversity that DPA can achieve to ensure the gain is significant.

This paper is organized as follows. Section II describes the MIMO-OFDM system model with spatial multiplexing and the feedback channels. Section III describes pilot allocation framework and formulates a DFT-based channel estimation scheme. The derivation of a DPA algorithm for linear, SIC, and ML receivers is then discussed, as well as the MIPS algorithm in Section IV. Section V presents the SVQ scheme. The simulation results are provided in Section VI, and Section VII draws a conclusion.

II. MIMO-OFDM System Model with Spatial Multiplexing

We consider an uncoded spatial multiplexing MIMO-OFDM system with N_s subcarriers, N_t transmit and N_r receive antennas, where $N_t \leq N_r$ The received signals are organized in an $N_r N_s \times 1$ vector $\mathbf{y} = [\mathbf{y}_1, \ldots, \mathbf{y}_i, \ldots, \mathbf{y}_{N_r}]^T$ expressed by

$$\mathbf{y} = \mathbf{H}_{df}\mathbf{s} + \mathbf{v}, \tag{1}$$

where $\mathbf{H}^i$ is a $N_rN_s \times N_tN_s$ matrix:

$$\mathbf{H}_{df} = \begin{bmatrix} \mathbf{H}_{df}^{11} & \mathbf{H}_{df}^{21} & \dots & \mathbf{H}_{df}^{N_t1} \\ \mathbf{H}_{df}^{12} & \mathbf{H}_{df}^{22} & \dots & \vdots \\ \vdots & \vdots & \mathbf{H}_{df}^{ij} & \vdots \\ \vdots & \vdots & \ddots & \vdots \\ \mathbf{H}_{df}^{1N_r} & \mathbf{H}_{df}^{2N_r} & \dots & \mathbf{H}_{df}^{N_tN_r} \end{bmatrix}. \tag{2}$$

The matrix $\mathbf{H}_{df}^{ij}$ is a $N_s \times N_s$ diagonal matrix in $\mathbf{H}_{df}$ that represents the frequency selective channel between the ith transmit antenna and the jth receive antenna, so the channel frequency response is given as

$$\begin{aligned} &\mathbf{H}_{df}^{ij} = \text{diag}\{\mathbf{F}_L\mathbf{h}_{tl}^{ij}\} = \text{diag}\{\mathbf{h}_{df}^{ij}\} \\ &i = 1, 2, \dots, N_t, \quad j = 1, 2, \dots, N_r, \end{aligned} \tag{3}$$

where diag$\{\}$ represents a diagonal matrix constructed by the corresponding vector. The vector $\mathbf{h}_{tl}^{ij}$ denotes the length L channel impulse response vector $\mathbf{h}_{tl}^{ij} = [h_{tl}^{ij}(0), h_{tl}^{ij}(1), \dots, h_{tl}^{ij}(L-1)]^T$ between the ith transmit antenna and the jth receive antenna, which is modelled as a tapped delay line. Each entry in the vector can be modelled as an independent identically distributed (i.i.d.) complex Gaussian random variable with $\mathcal{CN}(0, \sigma^2_{h_{tl}^{ij}(l)})$. Additionally, the channel is assumed to experience quasi-static fading, which remain constant during one OFDM symbol. The power delay profile for any transmit and receive antenna pair is the same. Given the prior assumptions, the correlation matrix can be represented as $\mathbf{R}_c = \mathbf{F}_L\mathbb{E}\{\mathbf{h}_{tl}^{ij}\mathbf{h}_{tl}^{ij^H}\}\mathbf{F}_L$. Hence, the kth subcarrier's channel frequency response $h_{df}^{ij}(k)$ can be also modelled as $\mathcal{CN}(0, \sigma^2_{h_{df}^{ij}(k)})$, where $\sigma^2_{h_{df}^{ij}(k)} = \sum_{l=0}^{L-1} \sigma^2_{h_{tl}^{ij}(l)} = 1$. The matrix $\mathbf{F}_L$ is the first L columns of the $N_s \times N_s$ DFT matrix. A feedback line is assumed to be perfect and instantaneous unless otherwise specified.

III. DFT-BASED CHANNEL ESTIMATION FOR MIMO-OFDM SYSTEMS

In this section, the DFT-based channel estimation and pilot allocation for MIMO-OFDM are discussed, and channel estimation errors for particular pilot patterns have been derived for the following optimization metrics.

A. Pilot Allocation with Multiple Transmit Antennas

A lattice-type pilot pattern is utilized in the space-frequency domain [7]. The ith transmit antenna pilot pattern can be represented by a $N_s \times N_s$ diagonal matrix $\mathbf{P}_i$ in which $1s$ denote the pilot subcarriers, and $0s$ are used for data or null subcarriers.

$$\mathbf{P}_i = \begin{bmatrix} 1 & 0 & \dots & 0 \\ 0 & 0 & \dots & \vdots \\ \vdots & \vdots & \ddots & \vdots \\ 0 & 0 & \dots & 1 \end{bmatrix} \qquad i = 1, 2, \dots, N_t, \tag{4}$$

where $\mathbf{P}_i \in \mathcal{P}$, $\|\mathcal{P}\| = \begin{pmatrix} N_s - (i-1)N_p \\ \\ N_p \end{pmatrix}$, $tr\{\mathbf{P}_i\} = N_p$, $\forall\, i$, and $\mathcal{P}$ denotes the set of all possible combinations of pilot allocation. The matrix in (4) represents one particular example of a pilot allocation matrix for the ith antenna.

B. DFT-based Channel Estimation

Since the pilot subcarriers for the ith transmit antenna are interference free, we use 1 as the pilot symbols in the pilot allocation matrix $\mathbf{P}_i$ to obtain the channel in the frequency domain $\widehat{\mathbf{H}}_{df}^{ij}$ between the ith transmit antenna and the jth receive antenna. The received pilot signals for the jth receive antenna can be described as

$$\mathbf{r}_j^{(\text{pilot})} = \mathbf{P}_i \mathbf{F}_L \mathbf{h}_{tl}^{ij} + \mathbf{P}_i \mathbf{v}_j, \tag{5}$$

where $\mathbf{r}_j^{(\text{pilot})} = \mathbf{P}_i \mathbf{r}_j$, and $\mathbf{r}_j$ and $\mathbf{v}_j$ denote the received signals and noise for the jth receive antenna, respectively. The CIR can be computed using LS estimation [12], and the channel frequency response (CFR) estimates can be obtained by transformation of the CIR:

$$\begin{aligned} \widehat{\mathbf{h}}_{tl}^{ij} &= (\mathbf{P}_i \mathbf{F}_L)^{\dagger} \mathbf{r}_j^{(\text{pilot})} = (\mathbf{F}_L^H \mathbf{P}_i \mathbf{F}_L)^{-1} \mathbf{F}_L^H \mathbf{P}_i \mathbf{r}_j^{(\text{pilot})}, \\ \widehat{\mathbf{H}}_{df}^{ij} &= \text{diag}(\mathbf{F}_L (\mathbf{F}_L^H \mathbf{P}_i \mathbf{F}_L)^{-1} \mathbf{F}_L^H \mathbf{P}_i \mathbf{r}_j^{(\text{pilot})}), \end{aligned} \tag{6}$$

where $L \leq N_p$. After some manipulation with $\mathbf{r}_j^{(\text{pilot})}$, we obtain a mathematical expression for the CFR estimates by substituting (5) into (6)

$$\widehat{\mathbf{H}}_{df}^{ij} = \mathbf{H}_{df}^{ij} + \text{diag}(\mathbf{F}_L(\mathbf{F}_L^H\mathbf{P}_i\mathbf{F}_L)^{-1}\mathbf{F}_L^H\mathbf{P}_i\mathbf{v}_j) = \mathbf{H}_{df}^{ij} + \mathbf{\Omega}_{ij}, \tag{7}$$

where $\mathbf{\Omega}_{ij}$ denotes the channel estimation errors between the ith transmit antenna and the jth receive antenna. Hence, the covariance matrix of $\widehat{\mathbf{H}}_{df}^{ij}$ can be represented as

$$\begin{aligned}\mathbb{E}\{\widehat{\mathbf{H}}_{df}^{ij}\widehat{\mathbf{H}}_{df}^{ij^H}\} &= \mathbb{E}\{\mathbf{H}_{df}^{ij}\mathbf{H}_{df}^{ij^H}\} + \mathbb{E}\{\mathbf{\Omega}_{ij}\mathbf{\Omega}_{ij}^H\} = \mathbb{E}\{\mathbf{H}_{df}^{ij}\mathbf{H}_{df}^{ij^H}\} + \sigma_v^2\text{diag}(\mathbf{F}_L(\mathbf{F}_L^H\mathbf{P}_i\mathbf{F}_L)^{-1}\mathbf{F}_L^H) \\ &= \mathbf{I}_{N_s} + \sigma_v^2\mathbf{\Xi}_{ij},\end{aligned} \tag{8}$$

where $\mathbf{\Xi}_{ij}$ denotes the covariance matrix of the channel estimation errors, which is determined by one particular pilot allocation matrix $\mathbf{P}_i$. Based on (7) and (8), the actual channel $\mathbf{H}_{df}^{ij}$ can be expressed in terms of the estimated channel $\widehat{\mathbf{H}}_{df}^{ij}$ as [13]

$$\mathbf{H}_{df}^{ij} = (\mathbf{I}_{N_s} + \mathbb{E}\{\mathbf{\Omega}_{ij}\mathbf{\Omega}_{ij}^H\})^{-1}\widehat{\mathbf{H}}_{df}^{ij} - \widetilde{\mathbf{\Omega}}_{ij} = (\mathbf{I}_{N_s} + \sigma_v^2\mathbf{\Xi}_{ij})^{-1}\widehat{\mathbf{H}}_{df}^{ij} - \widetilde{\mathbf{\Omega}}_{ij}, \tag{9}$$

In order to obtain the covariance matrix of $\widetilde{\mathbf{\Omega}}_{ij}$, equation (7) can be transformed as follows. Substituting (9) into (7), the expression becomes

$$\mathbf{\Omega}_{ij} - \widetilde{\mathbf{\Omega}}_{ij} = (\mathbf{I}_{N_s} + \sigma_v^2\mathbf{\Xi}_{ij})^{-1}\sigma_v^2\mathbf{\Xi}_{ij}\widehat{\mathbf{H}}_{df}^{ij}, \tag{10}$$

so

$$\widetilde{\mathbf{\Omega}}_{ij} = \mathbf{\Omega}_{ij} - (\mathbf{I}_{N_s} + \sigma_v^2\mathbf{\Xi}_{ij})^{-1}\sigma_v^2\mathbf{\Xi}_{ij}\widehat{\mathbf{H}}_{df}^{ij}. \tag{11}$$

It can be found that $\mathbb{E}\{\widetilde{\mathbf{\Omega}}_{ij}\} = 0$, and the covariance matrix of $\widetilde{\mathbf{\Omega}}_{ij}$ is given by

$$\begin{aligned}\mathbb{E}\{\widetilde{\mathbf{\Omega}}_{ij}\widetilde{\mathbf{\Omega}}_{ij}^H\} &= \sigma_v^2\mathbf{\Xi}_{ij} - 2(\mathbf{I}_{N_s} + \sigma_v^2\mathbf{\Xi}_{ij})^{-1}\sigma_v^2\mathbf{\Xi}_{ij}\sigma_v^2\mathbf{\Xi}_{ij}^H + (\mathbf{I}_{N_s} + \sigma_v^2\mathbf{\Xi}_{ij})^{-1}\sigma_v^2\mathbf{\Xi}_{ij}\sigma_v^2\mathbf{\Xi}_{ij}^H \\ &= (\mathbf{I}_{N_s} + \sigma_v^2\mathbf{\Xi}_{ij})^{-1}\sigma_v^2\mathbf{\Xi}_{ij}.\end{aligned} \tag{12}$$

From (9), the actual channel can be approximated by the estimated channel, which corresponds to one particular pilot pattern. In the following section, equation (9) will be used to calculate the SINR or MSE and the corresponding SER estimates, which correspond to different pilot patterns. Then, the optimum pilot pattern can be chosen based on the SER estimates.

IV. Dynamic Pilot Allocation for MIMO Receivers and MIMO Iterative Pilot Search

In this section, we derive DPA using (9) for different receivers with BPSK modulation. The same strategy can also be extended to other receiver techniques such as [14] with other modulation schemes.

A. Dynamic Pilot Allocation Algorithm for Linear and SIC Receivers

For linear and SIC receivers, the SINR is used for the SER estimates. Due to channel estimation errors, inter-antenna interference and noise, the expression of the detected symbols for the qth desired transmit antenna currently being processed is obtained by substituting (9) into the system model described in (1):

$$\begin{aligned}\widehat{\mathbf{s}}_q = \widehat{\mathbf{W}}^q_{\text{linear}}\mathbf{y} = &\underbrace{\widehat{\mathbf{W}}^q_{\text{linear}}(\mathbf{I}_{N_rN_s} + \sigma_v^2\boldsymbol{\Xi}_q)^{-1}\widehat{\mathbf{H}}^q_{df}\mathbf{s}_q}_{\text{signals}} - \underbrace{\widehat{\mathbf{W}}^q_{\text{linear}}\widetilde{\boldsymbol{\Omega}}_q\mathbf{s}_q}_{\text{channel estimation error}} \\ &\underbrace{- \widehat{\mathbf{W}}^q_{\text{linear}}\sum_{i=1}^{d-1}(\mathbf{I}_{N_rN_s} + \sigma_v^2\boldsymbol{\Xi}_i)^{-1}\sigma_v^2\boldsymbol{\Xi}_i\widehat{\mathbf{H}}^i_{df}\widehat{\mathbf{s}}_i}_{\text{residual interference}} \\ &\underbrace{+ \widehat{\mathbf{W}}^q_{\text{linear}}\sum_{\substack{i=d\\ i\neq q}}^{N_t}(\mathbf{I}_{N_rN_s} + \sigma_v^2\boldsymbol{\Xi}_i)^{-1}\widehat{\mathbf{H}}^i_{df}\mathbf{s}_i}_{\text{inter-antenna interference}} - \underbrace{\widehat{\mathbf{W}}^q_{\text{linear}}\sum_{\substack{i=1\\ i\neq q}}^{Nt}\widetilde{\boldsymbol{\Omega}}_i\mathbf{s}_i}_{\text{channel estimation error}} + \underbrace{\widehat{\mathbf{W}}^q_{\text{linear}}\mathbf{v}}_{\text{noise}}, \qquad q = 1, \ldots, N_t\end{aligned} \tag{13}$$

where $\widehat{\mathbf{H}}^i_{df} = [\widehat{\mathbf{H}}^{i1}_{df} \ldots \widehat{\mathbf{H}}^{ij}_{df} \ldots \widehat{\mathbf{H}}^{iN_r}_{df}]^T$, $\boldsymbol{\Xi}_i = \text{diag}\{\boldsymbol{\Xi}_{i1} \ldots \boldsymbol{\Xi}_{ij} \ldots \boldsymbol{\Xi}_{iN_r}\}$, $\widetilde{\boldsymbol{\Omega}}_i = [\widetilde{\boldsymbol{\Omega}}_{i1} \ldots \widetilde{\boldsymbol{\Omega}}_{ij} \ldots \widetilde{\boldsymbol{\Omega}}_{iN_r}]^T$, and the MMSE filter for the qth transmit antenna given on the channel estimates in (6) can be given by

$$\widehat{\mathbf{W}}^q_{\text{linear}} = (\widehat{\mathbf{H}}^{q^H}_{df}\widehat{\mathbf{H}}^q_{df} + \sum_{\substack{i=d\\ i\neq q}}^{N_t}\widehat{\mathbf{H}}^{i^H}_{df}\widehat{\mathbf{H}}^i_{df} + \sigma_v^2\mathbf{I}_{N_s})^{-1}\widehat{\mathbf{H}}^{q^H}_{df}. \tag{14}$$

Note that the value of d distinguishes the mathematical expressions of the linear receiver ($d = 1$) and the SIC receiver ($d = q$). Let $(\mathbf{I}_{N_rN_s} + N_0\boldsymbol{\Xi}_i)^{-1} = \Lambda_i$ and $(\mathbf{I}_{N_rN_s} + N_0\boldsymbol{\Xi}_i)^{-1}\sigma_v^2\boldsymbol{\Xi}_i = \tilde{\Lambda}_i$. Hence, the signal power $\boldsymbol{\gamma}^q_s$ for the qth transmit antenna can be calculated according to (13), which is

$$\boldsymbol{\gamma}^q_S = \mathcal{D}(\widehat{\mathbf{W}}^q_{\text{linear}}\Lambda_q\widehat{\mathbf{H}}^q_{df}\widehat{\mathbf{H}}^{q^H}_{df}\Lambda^H_q\widehat{\mathbf{W}}^{q^H}_{\text{linear}}), \tag{15}$$

where $\mathcal{D}()$ denotes the operation which extracts the diagonal elements of a matrix. Hence, $\boldsymbol{\gamma}^q_S = [\gamma^q_S(0), \ldots, \gamma^q_S(k), \ldots 1)]^T$. Similarly, the interference power for the qth transmit antenna can be approximated by

$$\boldsymbol{\gamma}^q_I = \mathcal{D}(\sum_{i=1}^{d-1}\widehat{\mathbf{W}}^q_{\text{linear}}\tilde{\Lambda}_i\widehat{\mathbf{H}}^i_{df}\widehat{\mathbf{H}}^{i^H}_{df}\tilde{\Lambda}^H_i\widehat{\mathbf{W}}^{q^H}_{\text{linear}} + \sum_{\substack{i=d\\ i\neq q}}^{N_t}\widehat{\mathbf{W}}^q_{\text{linear}}\Lambda_i\widehat{\mathbf{H}}^q_{df}\widehat{\mathbf{H}}^{i^H}_{df}\Lambda^H_i\widehat{\mathbf{W}}^{q^H}_{\text{linear}}). \tag{16}$$

Similar to $\boldsymbol{\gamma}_S^q$, $\boldsymbol{\gamma}_I^q = [\gamma_S^q(0), \ldots, \gamma_I^q(k), \ldots, \gamma_I^q(N_s-1)]^T$. Accordingly, the power of noise plus channel estimation errors can be given as

$$\boldsymbol{\gamma}_N^q = \mathcal{D}(\sum_{i=1}^{N_t} \widehat{\mathbf{W}}_{\text{linear}}^q \tilde{\Lambda}_i \widehat{\mathbf{W}}_{\text{linear}}^{qH} + \sigma_v^2 \widehat{\mathbf{W}}_{\text{linear}}^{qH} \widehat{\mathbf{W}}_{\text{linear}}^q), \tag{17}$$

where $\boldsymbol{\gamma}_N^q = [\gamma_N^q(0), \ldots, \gamma_N^q(k), \ldots, \gamma_N^q(N_s-1)]^T$. Hence, the SINR for the kth subcarrier can be written as

$$\text{SINR}_q(k) = \frac{\gamma_S^q(k)}{\gamma_N^q(k) + \gamma_I^q(k)}, \tag{18}$$

and the SER estimate for the kth subcarrier can be obtained by [15]

$$\mathbb{P}_q(k) \approx 2\mathcal{Q}(\sqrt{2\,\text{SINR}_q(k)}\sin(\pi/M)), \tag{19}$$

where $\mathcal{Q}$ denotes the Q-function, which is $\mathcal{Q}(a) = (2\pi)^{-1/2}\int_a^\infty e^{-f^2/2}df$ [15]. Corresponding to a particular pilot pattern matrix $\mathbf{P}_q$, the average SER estimates for the data subcarriers of the qth antenna can be represented as

$$\mathbb{P}_q(\mathbf{P}_q) \approx \frac{2}{N_d}\sum_{k=1}^{N_d} \mathcal{Q}(\sqrt{2\,\text{SINR}_q(k)}\sin(\pi/M)), \tag{20}$$

where the quantity N_d denotes the number of data subcarriers. Hence, the optimum pilot allocation can be obtained by solving the following optimization problem:

$$\mathbf{P}_q^{\text{opt}} = \underset{\mathbf{P}_q \in \mathcal{C}}{\text{argmin}}\, \mathbb{P}_q(\mathbf{P}_q). \tag{21}$$

Note that the optimum pilot allocation for the transmit antennas would be obtained using an exhaustive joint search in the space and frequency domains, but this is impractical for any scenario.

B. Dynamic Pilot Allocation for ML Receivers

In order to simplify the description, the ML receiver is efficiently implemented subcarrier by subcarrier. The SER estimates for ML receivers at the kth subcarrier can be approximated in a looser form as [**?**], [16], [18]

$$\mathbb{P}(k) \le N_r(|\mathbb{C}|-1)\mathcal{Q}\left(\sqrt{\frac{\frac{1}{N_t}d_{min}^2(\mathbf{H}(k))}{2\sigma_v^2}}\right), \tag{22}$$

where

$$d^2_{min}(\mathbf{H}(k)) = \underset{\substack{\mathbf{s}(k),\mathbf{s}'(k)\in\mathbb{C}^{N_t} \\ \mathbf{s}(k)\neq\mathbf{s}'(k)}}{\operatorname{argmin}} \frac{\|\mathbf{H}(k)(\mathbf{s}(k)-\mathbf{s}'(k))\|^2}{N_t}. \tag{23}$$

Note that the SER estimates for ML receiver cannot be easily approximated using SINR as linear and SIC receivers. In the following, a special MSE based SER approximation is used. where $\mathbf{y}(k) = [y_1(k), \ldots, y_j(k), \ldots, y_{N_r}(k)]^T$ and $\mathbf{s}(k) = [s_1(k), \ldots, s_j(k), \ldots, s_{N_r}(k)]^T$ denote the receive and transmit signal vectors corresponding to the kth subcarrier. The channel matrix for the kth subcarrier is defined as $\mathbf{H}(k)$. Equation (22) has been verified as union bound in [18]. However, the complexity of the SER approximation is too high. An alternative method using a lower bound approximation (LBA) of (23) is considered in [16], but it suffers a performance loss. In order to obtain reliable SER estimates, the method proposed in [19], which reduce the complexity of searching $d^2_{min}(\mathbf{H}(k))$. Equation (9) cannot be simply substituted into (22), so it must be reformulated as

$$\mathbf{h}_q(k) = (\mathbf{I}_{N_t} + \sigma_v^2 \mathbf{\Xi}_q(k))^{-1} \widehat{\mathbf{h}}_q(k) - \widetilde{\boldsymbol{\omega}}_q(k). \tag{24}$$

where $\mathbf{h}_q(k) = [h_{q1}(k), \ldots, h_{qj}(k), \ldots, h_{qN_r}(k)]^T$ denotes the qth column of $\mathbf{H}(k)$, $\widetilde{\boldsymbol{\omega}}_q(k) = [\Omega_{q1}(k), \ldots, \Omega_{qj}(k), \ldots, \Omega_{qN_r}(k)]^T$ and $\widetilde{\Omega}_{qj}(k)$ denotes the kth diagonal element of $\widetilde{\mathbf{\Omega}}_{qj}$, and $\mathbf{\Xi}_q(k) = \text{diag}(\Xi_{q1}(k), \ldots, \Xi_{qj}(k), \ldots, \Xi_{qN_r}(k))$ and $\Xi_{qj}(k)$ denotes the kth diagonal element of $\mathbf{\Xi}_{qj}$. Substituting (24) into (22), we can obtain the SER approximation for the qth transmit antenna as

$$\mathbb{P}_q(k) \approx \sum_{k=1}^{N_s} N_r(M-1)\mathcal{Q}\left(\sqrt{\frac{\frac{1}{N_t}d^2_{min}(\mathbf{H}(k))}{2\sigma_v^2}}\right), \tag{25}$$

Equation (25) is defined as the same as (19). Hence, the optimization problem of ML receiver is identical to that of the linear and SIC receivers in (21). Note that the SER estimates of pilot and data subcarriers must be jointly optimized in order to obtain acceptable channel estimates.

C. SER v.s. MSE

In order to show the differences between the SER metric and the MSE metric used for pilot allocation, we derive the MSE metric using linear and SIC receivers for DPA as follows. Note that the ML receivers

use a special MSE metric.

$$\begin{aligned}
\mathrm{MSE}_q &= \mathbb{E}\{\|\mathbf{s}_q - \widehat{\mathbf{W}}^q_{\text{linear}}\mathbf{y}\|^2\} \\
&= \mathbb{E}\{\mathbf{I}_{N_s} - 2\widehat{\mathbf{W}}^q_{\text{linear}}\widehat{\mathbf{H}}^q_{df} + \widehat{\mathbf{W}}^q_{\text{linear}}\sum_{i=d,i\neq q}^{N_t}\mathbf{H}^i_{df}\mathbf{H}^{iH}_{df}\widehat{\mathbf{W}}^{qH}_{\text{linear}} + \widehat{\mathbf{W}}^q_{\text{linear}}\sigma_v^2\widehat{\mathbf{W}}^{qH}_{\text{linear}}\} \\
&= \mathbb{E}\{-2\widehat{\mathbf{W}}^q_{\text{linear}}\mathbf{H}^q_{df} + \mathbf{\Phi}\} \\
&= \mathbb{E}\{-2\widehat{\mathbf{W}}^q_{\text{linear}}((\mathbf{I}_{N_rN_s} + \sigma_v^2\mathbf{\Xi}_q)^{-1}\widehat{\mathbf{H}}^q_{df} - \tilde{\mathbf{\Omega}}_q) + \mathbf{\Phi}\} \\
&= \mathbb{E}\{-2\widehat{\mathbf{W}}^q_{\text{linear}}(\mathbf{\Lambda}_q\widehat{\mathbf{H}}^q_{df} - \tilde{\mathbf{\Omega}}_q) + \mathbf{\Phi}\}
\end{aligned} \tag{26}$$

The term $\mathbf{\Phi}$ is a constant for any pilot pattern, which is determined by the pilot patterns of the other transmit antennas, so the minimization of (26) can be reduced to the maximization of $\widehat{\mathbf{W}}^q_{\text{linear}}(\mathbf{\Lambda}_q\widehat{\mathbf{H}}^q_{df} - \tilde{\mathbf{\Omega}}_q)$. For high SNR values, the term $\tilde{\mathbf{\Omega}}_q$ can be omitted for simplicity. This is because the term $\tilde{\mathbf{\Omega}}_q$ is determined by the noise, and is difficult to evaluate. Hence, the minimization of the MSE in (26) becomes the maximization of $\widehat{\mathbf{W}}^q_{\text{linear}}\mathbf{\Lambda}_q\widehat{\mathbf{H}}^q_{df}$, which is equivalent to the maximization of $\widehat{\mathbf{W}}^q_{\text{linear}}\mathbf{\Lambda}_q\widehat{\mathbf{H}}^q_{df}\widehat{\mathbf{H}}^{qH}_{df}\mathbf{\Lambda}^H_q\widehat{\mathbf{W}}^{qH}_{\text{linear}}$ in (15). It can be observed that the MSE metric is equivalent to a SINR metric at high SNR values. However, the better MSE, for uncoded system may be achieved due to the better MSE performance of some subcarriers, which does not mean the better overall SER for all data subcarriers. For low SNR values, the MSE metric cannot take the term $\tilde{\mathbf{\Omega}}_q$ into account, so the noise may cause the misplacements of the pilots. For coded systems, DPA can be considered as a method exploiting the frequency diversity or selection diversity, because it is highly likely to insert the pilots into the subcarriers with deep fading. Hence, the diversity gain of DPA will not be affected significantly with the aid of channel coding. As stated in [20], the BER performance of coded OFDM systems over frequency selective channels is better than that over less frequency selective channels. In other words, the coded OFDM systems with the use of DPA seems working over more frequency selective channels. Basically, DPA makes better use of pilots at the transmitter at the expense of less accurate channel estimates. For ML receiver based DPA, the SER performance, using the minimum Euclidean distance, is evaluated differently from the linear and SIC receivers, which can be considered as a special MSE representation.

D. Proposed MIMO Iterative Pilot Search

The MIPS algorithm proposes to reduce the complexity burden for optimum pilot allocation using an iterative search in the space-frequency domain. It is developed from the iterative pilot search for SISO-OFDM [11]. The main idea behind the iterative pilot search is to search for the optimum position for the pth pilot while fixing the other $N_p - 1$ pilots on particular subcarriers. The MIPS follows the same pattern for a given transmit antenna q, but the pilot placement for other antennas must be considered. Furthermore, the first allocated antennas have more available subcarriers to insert pilots compared to the other antennas, so we perform the ordering with the aid of the SER estimates from the previous OFDM symbol period $\mathbb{P}_i(n-1)$, which corresponds to the pilot allocation matrices $\mathbf{P}_i^{\text{opt}}(n-1), i = 1, \ldots, N_t$. Hence, the antenna with the highest SER estimates in the previous OFDM symbol is allocated first. In other words, it has more pilot allocation matrices to choose, so the SER performance has better chance to be improved. For SIC receiver, the ordering is determined by detection ordering, because the performance of first detected antenna is worse than the later detected ones in most cases. Note that the covariance matrix of the noise $\mathbf{\Xi}_{i,i\neq q}$ corresponding to a particular pilot allocation must be used in the calculation of SINR or MSE. We assume that $\mathbf{\Xi}_i[n] \approx \mathbf{\Xi}_i[n-1], i = q+1, \ldots, N_t$ for these unknown pilot patterns, in (18) and (24). The number of required trials for a conventional exhaustive search are given by $\prod_{i=1}^{N_t} \binom{N_s-(i-1)N_p}{N_p}$, but the MIPS can significantly decrease the number of trials to $\sum_{i=1}^{N_t}(N_s - iN_p + 1)N_p$. Note that most operations required in the search trials can be pre-computed to further save the computational efforts. The exact algorithm table is presented in Table I.

V. Limited Feedback for Dynamic Pilot Allocation

Although the MIPS can reduce the complexity of finding an optimum pilot allocation, the feedback payload is still high, and so is the number of search trials. The total number of overhead bits is $\sum_{i=0}^{N_t-1} \log_2 \binom{N_s-iN_p}{N_p}$. We therefore extend the use of DPA over limited feedback channels using a stacked vector quantization (SVQ) technique, which can create a codebook for the pilot allocation of all transmit antennas unlike MIPS to search the pilot patterns separately. The SVQ first transform all

TABLE I: MIPS for the qth transmit antenna

Input: $\mathbf{P}_i[n], i = 1, \ldots, q-1$, N_s, N_p

Output: $\mathbf{P}_q^{\text{opt}}$

$\mathbf{P}_q^{\text{opt}} \leftarrow \mathbf{P}_q[n-1]$

$\mathbf{P}_i \leftarrow \mathbf{P}_i[n], i = 1, \ldots, q-1$

$\mathbb{P}_{\text{in}} \leftarrow 10^6$

idx $\leftarrow$ the indices of the diagonal elements of $\mathbf{P}_q[n-1]$ that contain pilots

repeat

  $\mathbb{P}_{\text{out}} \leftarrow \mathbb{P}_{\text{in}}$

  for $p = 0$ **to** $N_p - 1$

    $\mathbf{P}_q \leftarrow \mathbf{P}_q^{\text{opt}}$

    $\mathbf{P}_q[\text{idx}[p]] \leftarrow 0$

    $\mathbb{P}_{in} \leftarrow 1$

    for $k \leftarrow 0$ to $\text{N}_\text{s} - 1$

      $\mathbf{P}_q = \mathbf{P}_q + \sum_{i=1}^{q-1} \mathbf{P}_i$

      if $\mathbf{P}_q[k] = 1$

        $\mathbf{P}_q = \mathbf{P}_q - \sum_{i=1}^{q-1} \mathbf{P}_i$

      then go back to 10

      else $\mathbf{P}_q[k] \leftarrow 1$

        $\mathbf{P}_q = \mathbf{P}_q - \sum_{i=1}^{q-1} \mathbf{P}_i$

        $\mathbb{P}_{\text{out}} = \mathbb{P}_q$ given on $\mathbf{P}_q$ in (20) or (25)

      end

      if $\mathbb{P}_{\text{out}} < \mathbb{P}_{\text{in}}$ **then**

        $\mathbb{P}_{\text{in}} \leftarrow \mathbb{P}_{\text{out}}$

        $\mathbf{P}_q^{\text{opt}} \leftarrow \mathbf{P}_q$

        idx[p] $\leftarrow$ k

      end

      $\mathbf{P}_q[k] \leftarrow 0$

    end

  end

until $\mathbb{P}_{in} < \mathbb{P}_{\text{out}}$

pilot allocation matrices into vectors and then stack these vectors in one vector for the generalized Lloyd algorithm (GLA) [21]. Furthermore, the proposed SVQ can also be efficiently implemented using multi-stage vector quantization schemes and correlation between OFDM symbols can be exploited using predictive vector quantization schemes [23]. The SVQ jointly quantizes the optimum pilot allocation set. Thus the approximation $\widetilde{\mathbf{\Omega}}_{i,i\neq q}[n] \approx \widetilde{\mathbf{\Omega}}_{i,i\neq q}[n-1]$ can be replaced by the actual $\widetilde{\mathbf{\Omega}}_{i,i\neq q}[n]$ in the SINR or MSE calculation, because the possible pilot patterns of all transmit antennas are already known. The algorithm is provided in Table II.

TABLE II: SVQ for optimum pilot allocation

Input: $\mathcal{B}, Q$

Output: $\mathcal{B}_Q$

Choose initial codebook $\mathcal{B}_0$ from $\mathcal{B}$

for $q = 1$**:**Q

$\mathcal{B}_q = \mathcal{B}_{q-1}$

for $n = 1$**:**N

$n'_{\text{min}} = \text{argmin}_{\overline{\mathbf{x}}^{opt}[n'] \in \mathcal{B}_q} \|\mathbf{x}^{opt}[n] - \overline{\mathbf{x}}^{opt}[n']\|_F^2$

$\mathcal{V}_{n'_{\text{min}}} = \mathbf{x}^{opt}[n'_{\text{min}}] + \mathcal{V}_{n'_{\text{min}}}$ (the n'_{min}th column of $\mathcal{V}$)

end

$\overline{\mathbf{x}}^{\text{opt}}[n'] = \frac{1}{|\mathcal{V}_{n'}|}\mathcal{V}_{n'}$

($|\mathcal{V}_{n'}|$ is the counter for n'th column of $\mathcal{V}$ in step 6)

Put $\overline{\mathbf{x}}^{opt}[n']$ in corresponding column of $\mathcal{B}_q$

end

Map the $\mathcal{B}_Q$ to a binary structure antenna by antenna, and exclude the previous antenna's pilot tones.

Set the N_p largest values to 1, and the rest to 0.

VI. Simulation Results

In this section, the DPA and UPA with different receivers (linear, SIC, ML) based on MIMO-OFDM systems are compared via Monte Carlo simulations. A diversity gain can be observed from these simulation results. Note that the performance difference between ZF and MMSE receivers may be negligible. In this case, we use MMSE receivers as linear and MMSE-SIC receivers as SIC. We assume a practical scenario with the following settings: the carrier frequency $f_c = 650$MHz, the subcarrier spacing $\Delta f = 976.5$Hz and the OFDM symbol duration $T = 1/\Delta f \approx 1$ms. The MIMO-OFDM system parameters are $L = 4, N_s = 32, N_p = 4, N_t = N_r = 2, 4$. The transmit signals are modulated with BPSK. Extension to other modulations is straightforward, by modify (20) and (25) as appropriate. We expect the result to be similar for such modulation. The channel estimation and detection performances are measured in terms of MSE and BER. The simulations are carried out over multipath channels with a uniform power delay profile and a normalized Doppler frequency $f_{\mathrm{d}}T_{\mathrm{OFDM}} = 10^{-4}$ unless otherwise specified. In other words, the channel varies slowly in terms of OFDM symbols. With a limited feedback channel, the simulation is performed in a scenario where the receivers relay back the small number of codebook indices, which implies that the feedback link can only send several bits. The codebook for the limited feedback channel can be determined in advance, with 2×10^4 initial OFDM symbol periods and 5 iterations at a given SNR (*e.g.* 25dB). Furthermore, WiFi is one possible application of DPA [26]. Firstly, it has a relatively limited number of subcarriers. Secondly, since DPA can improve the BER and SER, it could improve WiFi coverage. Thirdly, the channels experienced by WiFi users are slowly varying, and hence the diagonal channel matrix assumption is valid. Hence, DPA could be easily integrated with current WiFi schemes.

Fig. 1 depicts the BER and MSE performances of different receivers with DPA or UPA in a MIMO-OFDM system with $N_t = N_r = 2, N_s = 32, N_p = 4$ with BPSK. DPA with MIPS significantly outperforms the UPA in terms of BER around 10 dB at 10^{-3}, but gives poorer MSE performance. In other words, the system can achieve better BER performance at the expense of MSE degradation. The BER and MSE performances of DPA and UPA for ML receivers are also presented. From Fig. 1a, the DPA with lower bound approximation (LBA) of the SER estimates [16] performs worse than the DPA with the union

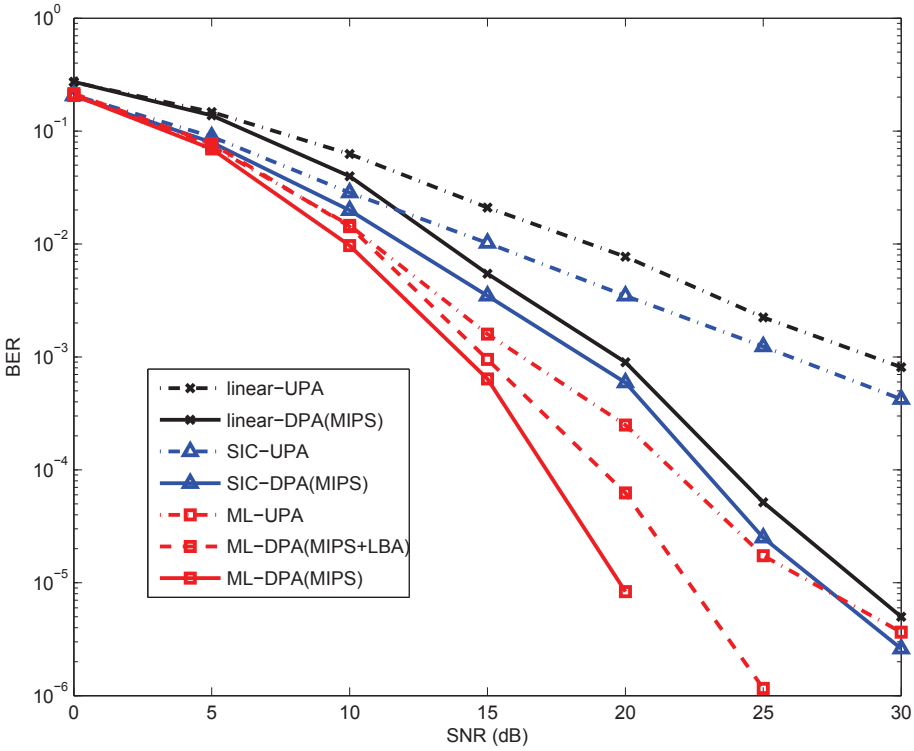

(a) BER

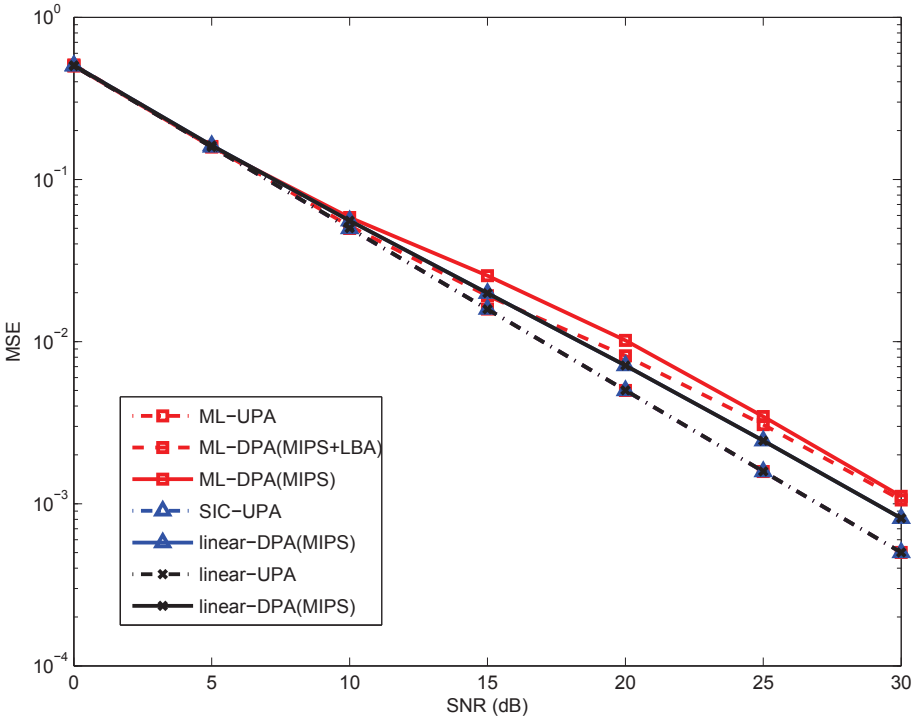

(b) MSE

Fig. 1: Comparison of BER and MSE between DPA and UPA for $N_t = N_r = 2, N_s = 32, N_p = 4, L = 4$

bound in (22) even at low SNR values. 5 dB BER performance gain can be obtained by DPA at high SNR. We then plot the DPA in a moderate size system with $N_t = N_r = 4, N_s = 32, N_p = 4$ modulated with BPSK in Fig. 2. The performance gains are still maintained for different receivers.

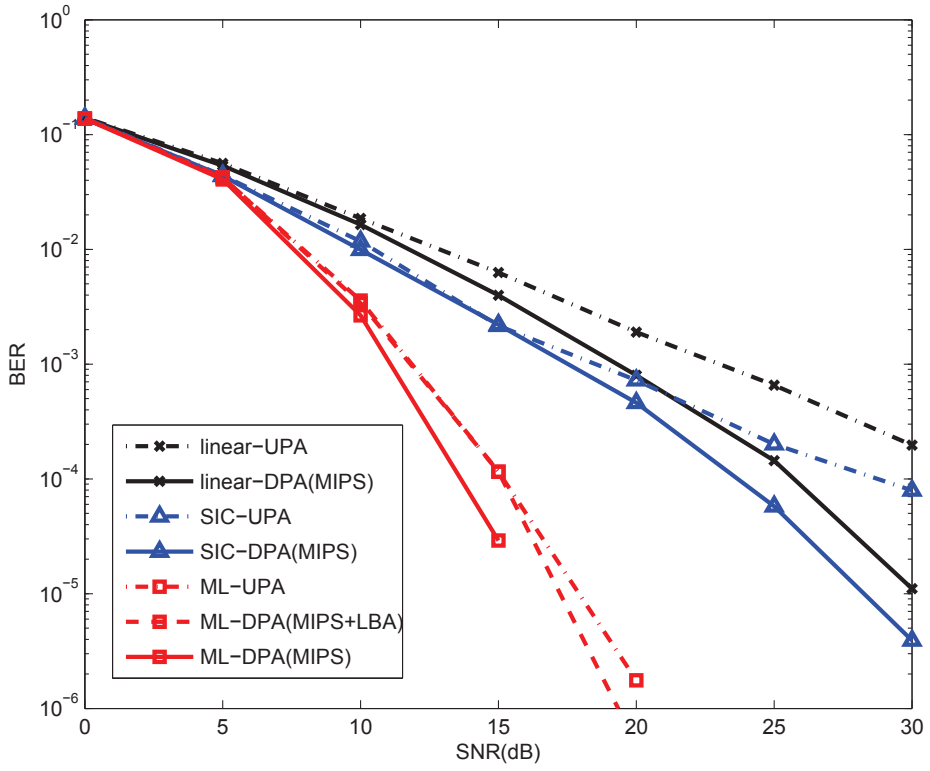

Fig. 2: Comparison of BER between DPA and UPA for $N_t = N_r = 4, N_s = 32, N_p = 4, L = 4$

In Fig. 3, the curves of BER performance against the number of feedback bits at SNR$=$ 15 dB are plotted to further illustrate the tradeoff between the number of feedback bits and the BER performance. Note that the complexity of DPA at the receiver is also reduced using a small number of feedback bits, which determines the number of search trials. According to our observation in Fig. 3 , an excellent tradeoff between complexity and performance gain can be achieved using 5 bits codebook. Hence, the feedback overhead is significantly reduced from 25 bits to several bits. The number of search trials is also reduced to a fixed number equal to 2^5.

The delay of the feedback link is assumed to be 20 ms (equivalent to 20 OFDM symbols), which is twice the length of the normal WiMAX feedback delay [24]. Because of the delay in the feedback

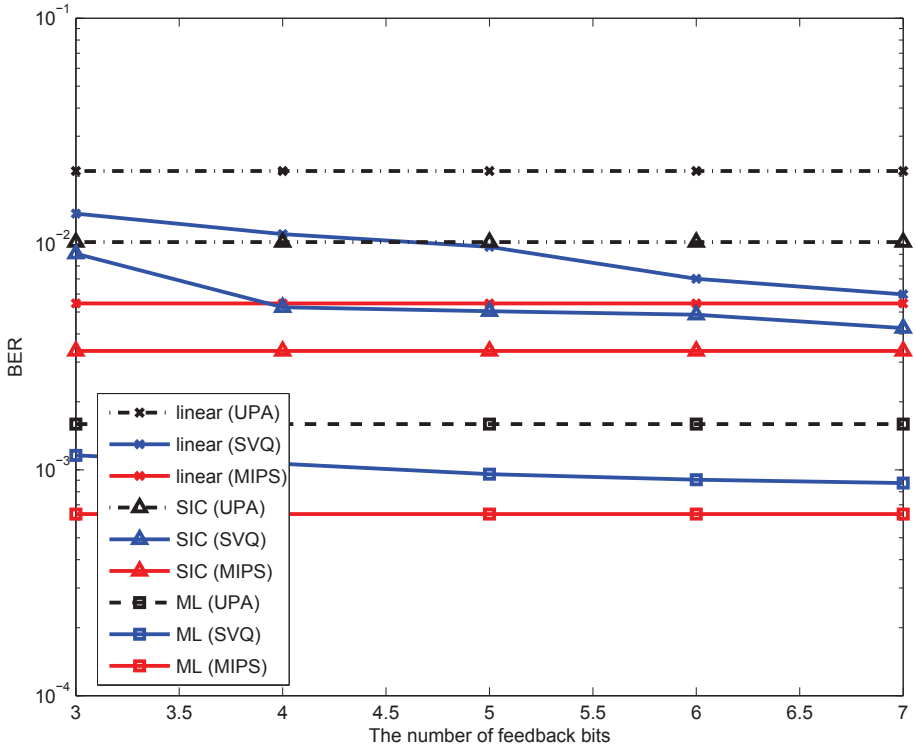

Fig. 3: Comparison of BER between different feedback bits with SVQ for $N_t = N_r = 2, N_s = 32, N_p = 4, L = 4$ at 15dB (The pilot positions for MIPS are perfectly known to the transmitter)

channel, the pilot allocation indices is not sent to the transmitter instantaneously, neither optimal. Here Fig. 4a details the BER performance of DPA over a range of $f_d T_{\text{OFDM}}$ with a fixed delay at SNR$=$ 20 dB . The performance of DPA is better than the UPA except for ML with SVQ-5 bits in a relatively slow varying channel with $f_d T_{\text{OFDM}}$ values between $f_d T_{\text{OFDM}} = 10^{-5}$ and $f_d T_{\text{OFDM}} = 3 - 4 \times 10^{-3}$. These are equivalent to a maximum relative velocity between the transmitter and receiver of around $3 - 4$ mph, which is sufficient for the pedestrians in most scenarios. In other words, the effect of increasing the feedback channel delay is negligible in slowly varying channels. Fig. 4b shows that the BER performance of DPA employing SVQ (5 bits) at SNR$=$ 15 dB when the feedback channel operates over a binary symmetric channel (BSC) with different error probabilities P_e. The feedback indices may be impaired by the errors, which cause the indices mismatch with the channels at the transmitter side. The BER performance degrades as we expect with the increasing error probabilities. Additionally, the linear and

SIC receivers are more robust to the feedback channel errors at very high P_e than ML receivers similar to ML receivers in Fig. 4a. This is because the SER estimates of ML receivers for DPA significantly rely on minimum Euclidean distance estimates in (22) that are more sensitive to the channel estimation errors introduced by the pilot allocation. However, DPA still outperforms UPA within an acceptable level of P_e. From Fig. 4, It can be observed that if the channel is varying rapidly, the errors of the feedback channel must be reduced to maintain the reliability of the already delayed indices.

In Fig. 5 , we present the BER performance of DPA using linear receivers with $L = 4$, $N_t = N_r = 2$ and $N_s = 32, N_p = 4, 6, 8, 10, 12, 14$ to illustrate the possible best diversity achieved by DPA. As shown above, the slopes of BER curves become steeper with the increasing number of pilots compared to UPA, because data avoid the faded subcarrier with DPA. DPA with perfect channel estimates can achieve a better performance. It may not only suggest that other receivers incorporating DPA can achieve a better performance, but also receivers with more advanced channel estimators will benefit from DPA much more than the channel estimators used above as similarly described in [11]. In order to further explain the performance improvement of DPA, we can introduce a simple diversity analysis. If the channels of subcarriers are uncorrelated, the upper bound of diversity order for linear receivers can be easily obtained as $d = L(N_t - N_r + 1)$ [25] without transmit antenna selection, which is not achievable for DPA. In our case, the exact diversity analysis becomes intractable due to the correlation. The BER slopes of DPA is mainly affected by N_p, and DPA is prone to select N_p subcarriers out of N_s. Hence, we consider the DPA as a special case of selection, but in the frequency domain rather than the space domain. Following similar rules in [25, Lemma 2], the achievable diversity equals $d = (L - \lceil(\frac{N_s - N_t N_p}{N_s})L\rceil + 1)(N_r - N_t + 1)$, which approximately agrees with the red curve in Fig. 5 with perfect CSI. The conclusion can also be naturally extended to other receivers such as SIC or ML. In general, the DPA exploits a selection diversity compared to UPA, the diversity of which can be further improved with the increase of N_p and more reliable channel estimates as in [11].

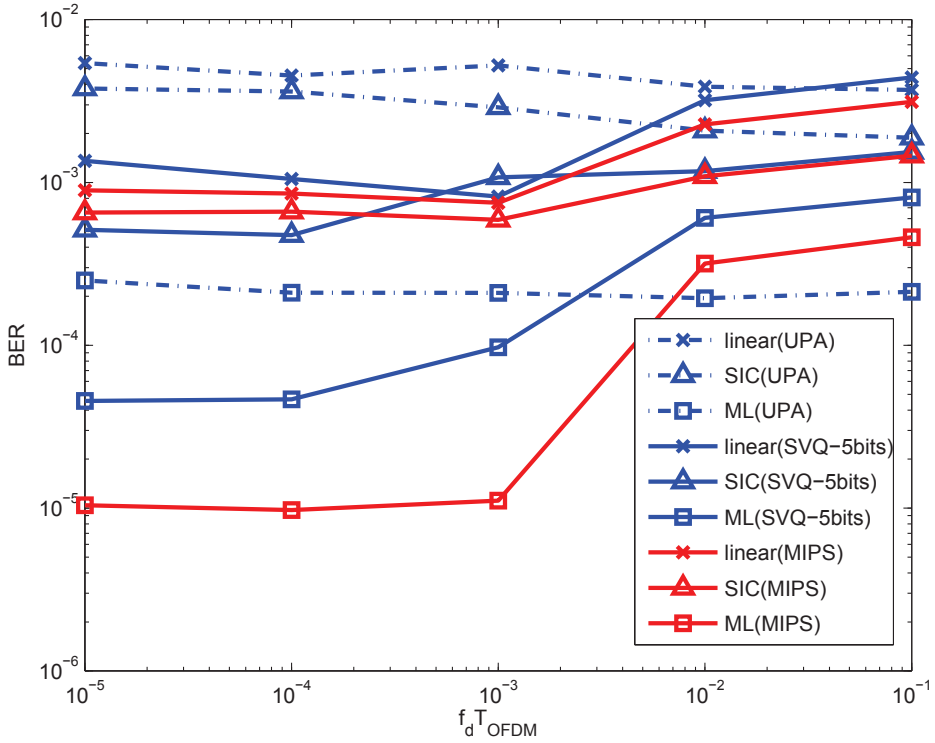

(a) Normalized Doppler frequency, SNR= 20 dB

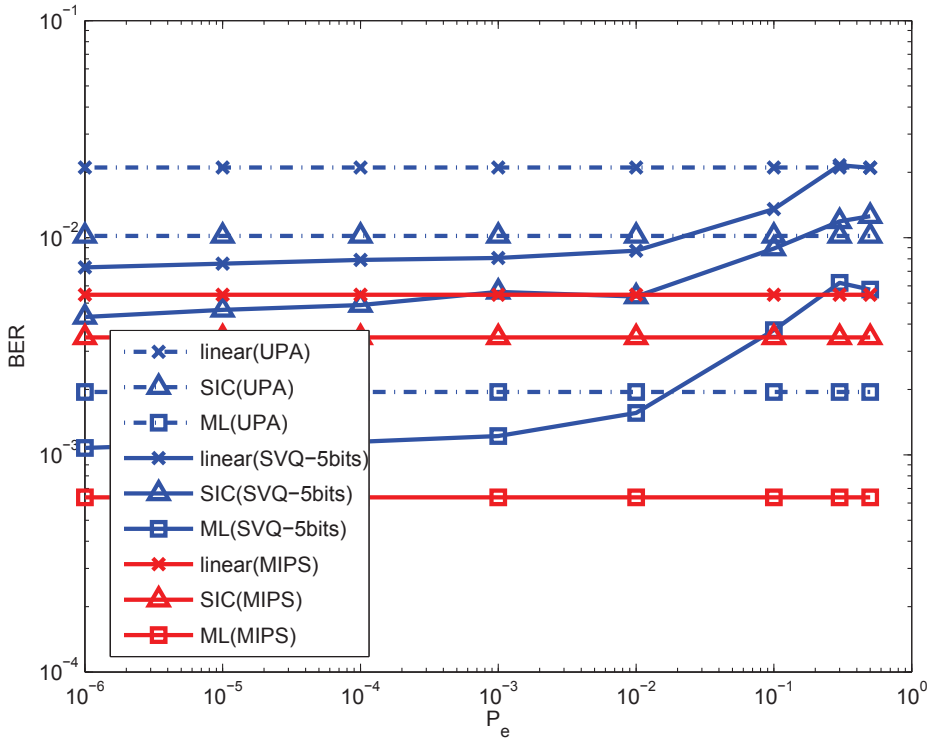

(b) Error probability of feedback channels $f_dT_{\mathrm{OFDM}} = 10^{-4}$, SNR= 15 dB

Fig. 4: Comparison of BER against f_dT_{OFDM} with a fixed feedback delay of 20 ms and P_e between DPA and UPA for $N_t = N_r = 2, N_s = 32, N_p = 4, L = 4$

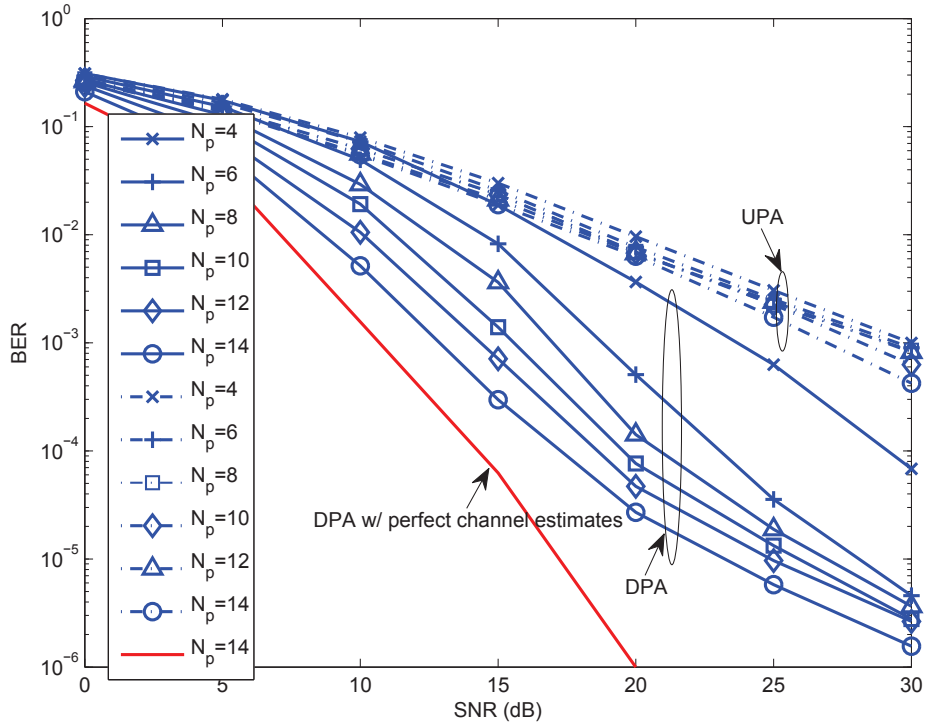

Fig. 5: Comparison of BER between DPA and UPA with different N_p for $N_t = N_r = 2, N_s = 32, L = 4$ with linear receivers

VII. Conclusion

A low-complexity dynamic pilot allocation has been derived for MIMO-OFDM systems (linear, SIC, ML), which can improve the SER performance at the expense of MSE degradation. DPA over a limited feedback channel has also been investigated, and a stacked vector quantization (SVQ) scheme has been proposed to reduce the feedback bits and the number of search trials for more practical scenarios. The gain of SER performance for DPA is promising over the limited feedback channels, and the time variation will not significantly affect the performance of DPA, if the channel is slow a time-varying channel. Finally, the achievable diversity of DPA with different receivers is discussed to further validate our simulation results. Hence, WiFi could incorporate DPA to improve the overall performance of MIMO-OFDM systems.

REFERENCES

[1] Li, Y., Cimini, L. J., Sollenberger, N. R.:'Robust channel estimation for OFDM systems with rapid dispersive fading channels', IEEE Trans. Commun., 1998, 46, (7), pp. 902-915

[2] Li, Y., Seshadri, N., Ariyavisitakul, S.: 'Channel estimation for OFDM systems with transmitter diversity in mobile wireless channels', IEEE J. Sel. Areas Commun., 1999, 17, (3), pp. 461-471

[3] Minn, H., Al-Dhahir, N.: 'Optimal training signals for MIMO OFDM channel estimation', IEEE Trans. Wireless Commun., 2006, 5, (5), pp. 1158-1168

[4] Barhumi, I., Leus, G., Moonen, M.:'Optimal training design for MIMO OFDM systems in mobile wireless channel', IEEE Trans. Signal Process., 2003, 51, (6), pp. 1615-1624

[5] Li, Y.:'Simplified channel estimation for OFDM systems with multiple transmit antennas', IEEE Trans. Wireless Commun., 2002, 1, (1), pp. 67-75

[6] Tuang, T.-L., Yao, K., Hudson, R. E.:'Channel estimation and adaptive power allocation for performance and capacity improvement of multiple-antenna OFDM systems'. Proc. IEEE Workshop on Signal Process. Adv. (SPAWC) 2001, Taiwan, ROC, Mar. 2001, pp. 82-85.

[7] Dowler, A., Doufexi, A., Nix, A.:'Performance evaluation of channel estimation techniques for a mobile fourth generation wide area OFDM systems'. Proc. IEEE Veh. Technol. Conf. (VTC) 2002, vol. 4, Vancouver, Canada, Sep. 2002, pp. 2036-2040.

[8] Chang, M. X.:'A new derivation of least-squares-fitting principle for OFDM channel estimation', IEEE Trans. Wireless Commun., 2006, 5, (4), pp. 726-731

[9] Morelli, M., Mengali,U.:'A comparison of pilot-aided channel estimation methods for OFDM systems', IEEE Trans. Signal Process., 2001, 49, (12), pp. 3065-3073

[10] Panah, A. Y., Vaughan, R. G., Heath, J. R. W.:'Optimizing pilot locations using feedback in OFDM systems', IEEE Trans. Veh. Technol., 2009, 58, (6), pp. 2803-2814

[11] Moraes, R. B., Sampaio-Neto, R.:'BER minimizing pilot symbol arrangement in closed-loop OFDM systems', IET Commun., 2011, 5, pp. 1999-2008

[12] Kay, S.:'Fundamentals of Statistical Signal Processing: Estimation Theory'(Prentice-Hall, 1993)

[13] Cai, X., Giannakis, G. B.:'Error probability minimizing pilots for OFDM with MPSK modulation over Rayleigh-fading channels', IEEE Trans. Veh. Technol., 2004, 53, (1), pp. 146-155

[14] de Lamare, R. C., Sampaio-Neto, R.:'Minimum mean square error iterative successive parallel arbitrated decision feedback detectors for DS-CDMA systems', IEEE Trans. Commun., 2008, 56, (5) pp. 778-789

[15] Simon, M., Alouini, M.:'Digital Communication Over Fading Channels: A Unified Approach to Performance Analysis'(Wiley, 2000)

[16] J. R. W. Heath, J. R. W., Paulraj, A. J.:'Switching between diversity and multiplexing in MIMO systems', IEEE Trans. Commun., 2005, 53, (6), pp. 963-968

[17] Zhu, X., and Murch, R. D.:'Performance analysis of maximum likelihood detection in a MIMO antenna system', IEEE Trans. Commun., 2002, 50, (2), pp. 187-191

[18] Goldsmith, A.:'Wireless Communications'(Cambridge, 2005.)

[19] Shin, M., Kang, J., Yoo, B., *et al*.:'An efficient searching algorithm for receive minimum distance in MIMO systems with ML receiver', IEICE Trans. Commun., 2009, E92-B, (1)

[20] Wessman, M.-O., Svensson, A., Agrell, E.:'Frequency diversity performance of coded multiband-OFDM systems on IEEE UWB channels'. Proc. IEEE Veh. Technol. Conf. (VTC) 2004 spring, vol. 2, Milan, Italy, Sep. 2004, pp. 1197-1201.

[21] Gersho, A., Gray, R.:'Vector Quantization and Signal Compression'(Kluwer, 1992)

[22] Linde, Y., Buzo, A., Gray, R.:'An algorithm for vector quantizer design', IEEE Trans. Commun., 1980, COM-28, (1), pp. 84-95

[23] de Lamare, R. C., Alcaim, A.:'Strategies to improve the performance of very low bit rate speech coders and application to a variable rate 1.2 kb/s codec', IEE Proc.- Vis. Image Signal Process., 2005, 152, (1), pp. 74-86

[24] Etemad, K., Lai, M.-Y.:'WiMAX Technology and Netwrok Evolution'(Wiley-IEEE Press, 2011)

[25] Zhang, H., Nabar, R. U.:'Transmit antenna selection in MIMO-OFDM systems: Bulk versus per-tone selection'. Proc. IEEE Int. Commun. Conf., Beijing, China, Apr. 2008. pp. 4371-4375

[26] IEEE 802.11n-2009:'Amendment 5: Enhancements for Higher Throughput '. IEEE-SA. 29 Oct. 2009.

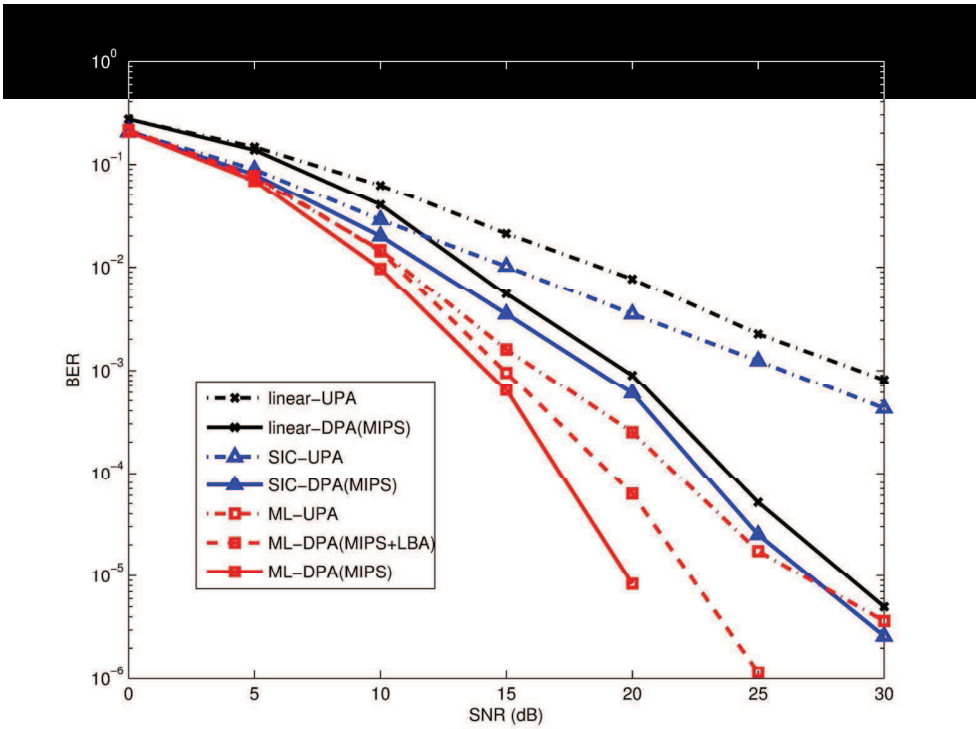

153x119mm (300 x 300 DPI)

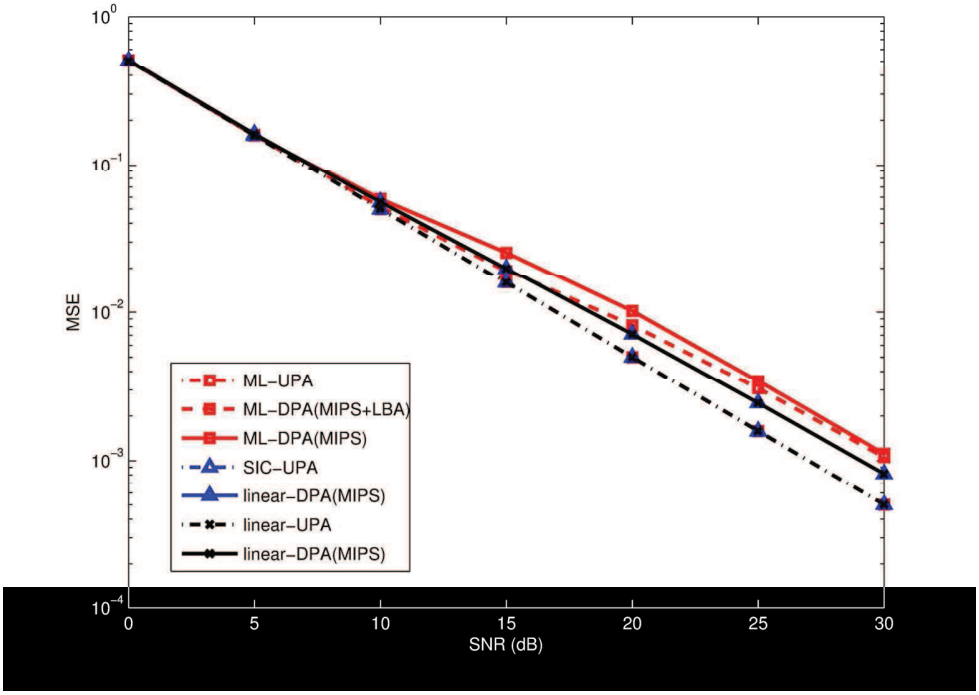

147x110mm (300 x 300 DPI)

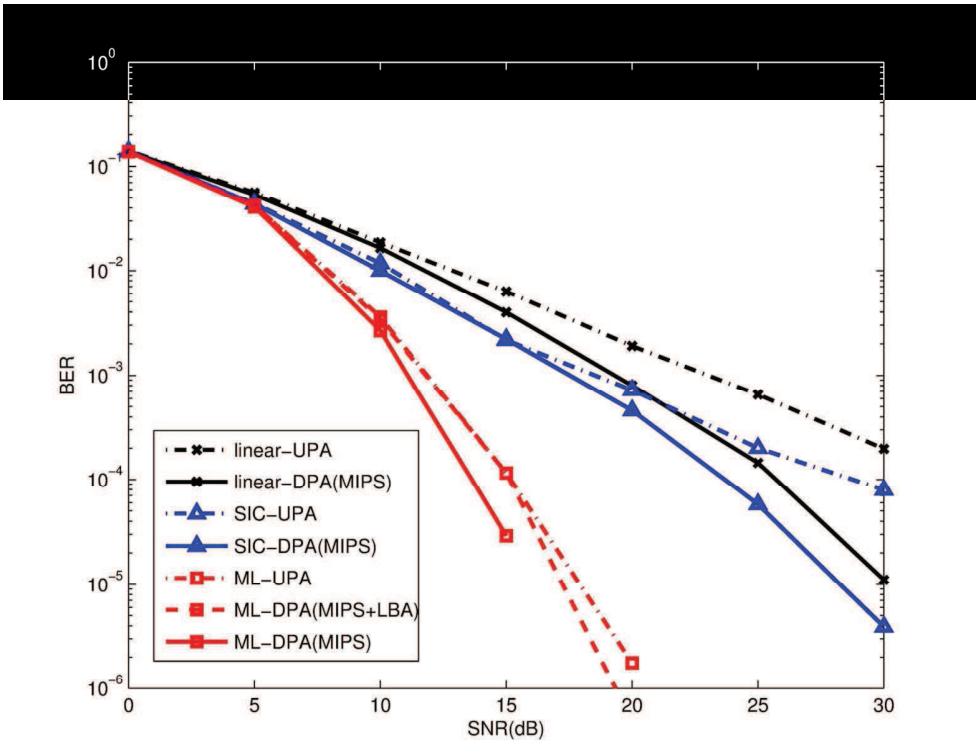

141x111mm (300 x 300 DPI)

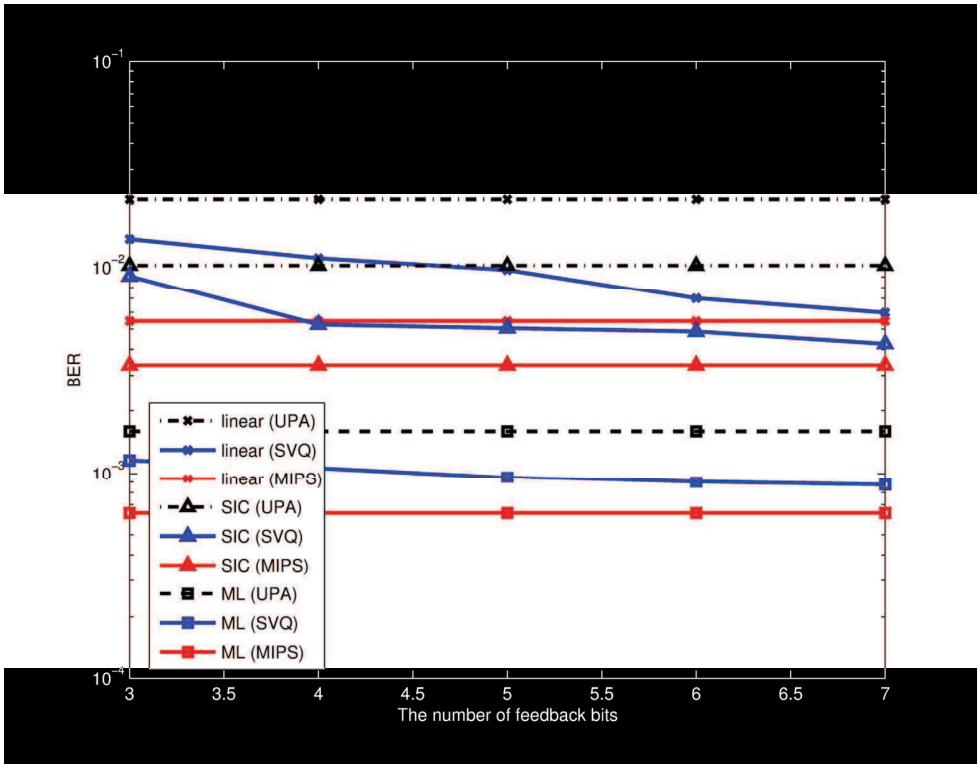

153x119mm (300 x 300 DPI)

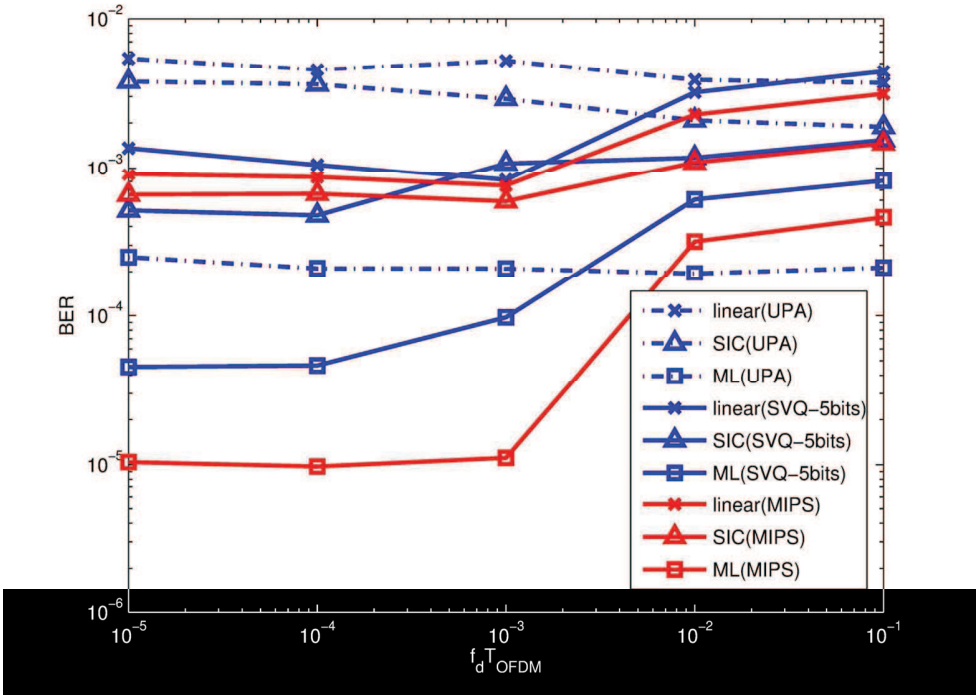

132x99mm (300 x 300 DPI)

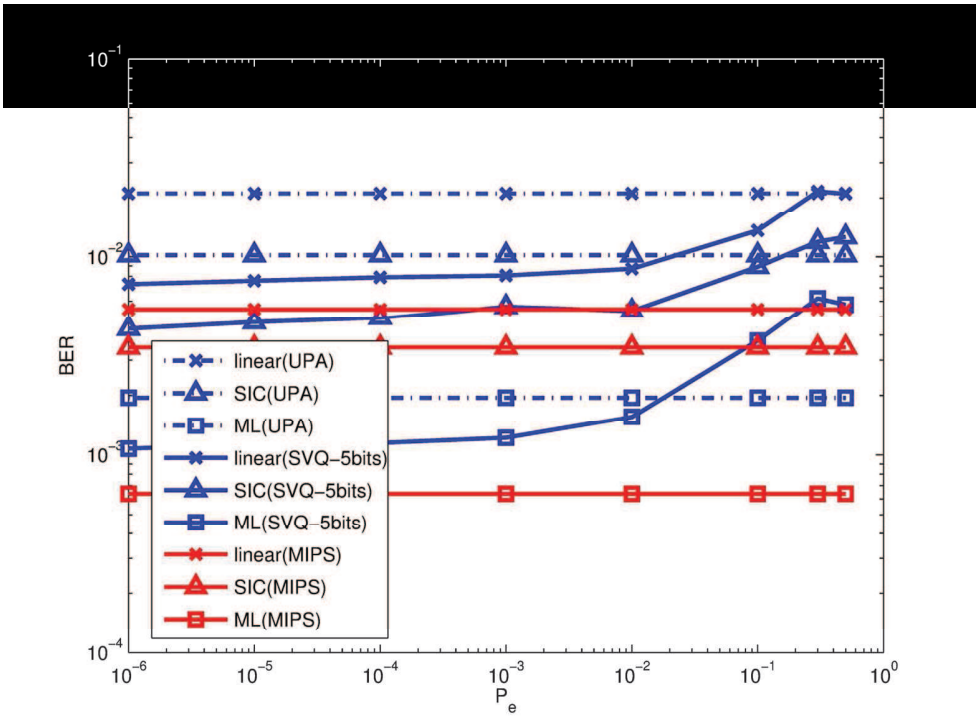

132x99mm (300 x 300 DPI)

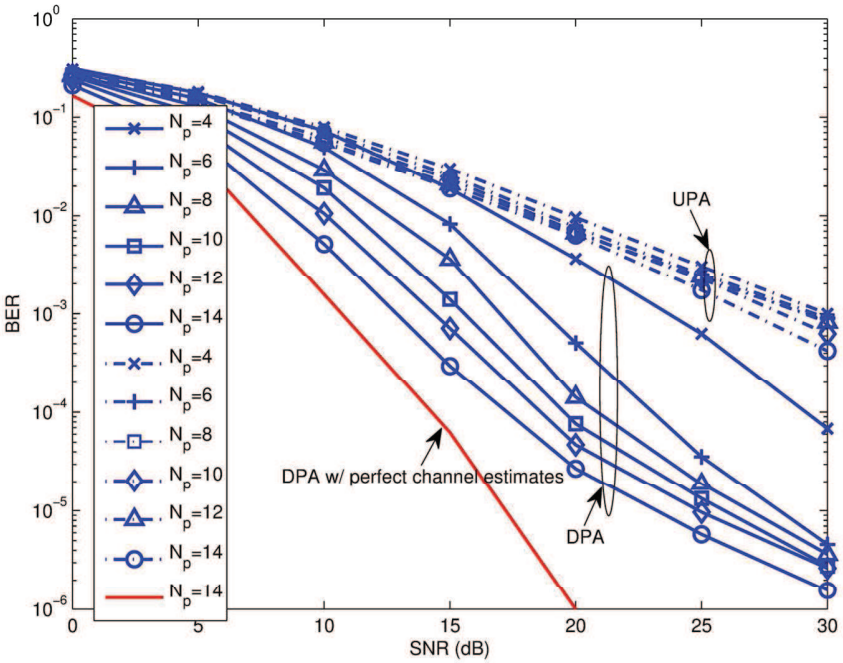

136x101mm (300 x 300 DPI)